

X-RAY EMITTING EJECTA OF SUPERNOVA REMNANT N132D

KAZIMIERZ J. BORKOWSKI,¹ SEAN P. HENDRICK,² & STEPHEN P. REYNOLDS¹

ABSTRACT

The brightest supernova remnant in the Magellanic Clouds, N132D, belongs to the rare class of oxygen-rich remnants, about a dozen objects that show optical emission from pure heavy-element ejecta. They originate in explosions of massive stars that produce large amounts of O, although only a tiny fraction of that O is found to emit at optical wavelengths. We report the detection of substantial amounts of O at X-ray wavelengths in a recent 100 ks *Chandra* ACIS observation of N132D. A comparison between subarcsecond-resolution *Chandra* and *Hubble* images reveals a good match between clumpy X-ray and optically emitting ejecta on large (but not small) scales. Ejecta spectra are dominated by strong lines of He- and H-like O; they exhibit substantial spatial variations partially caused by patchy absorption within the LMC. Because optical ejecta are concentrated in a 5 pc radius elliptical expanding shell, the detected ejecta X-ray emission also originates in this shell.

Subject headings: ISM: individual (N132D) — supernova remnants — X-rays: ISM — supernovae: general

1. INTRODUCTION

The heavy-element ejecta of core-collapse (CC) supernovae (SNe) are dominated by oxygen. By studying the properties of O and other freshly synthesized elements in supernova remnants (SNRs), we can infer the total amount of ejected O, relative abundances, and the spatial distribution of heavy elements. With this information, we can then constrain the progenitor main-sequence mass and learn more about how massive stars explode. Oxygen is most readily seen in X-rays, as evidenced by a growing number of O-rich SNRs detected by modern X-ray satellites such as *Chandra* and *XMM-Newton*. X-ray detection of plasma enriched in O but deficient in Fe allows us to identify CC SNRs in the first place. High-resolution studies of SNRs containing both optical and X-ray-emitting O ejecta hold particular promise for advancing our understanding of ejecta in CC SNRs.

N132D, an X-ray-bright SNR in the Large Magellanic Cloud (LMC), contains optically emitting O-rich ejecta (Sutherland & Dopita 1995; Morse et al. 1995, 1996). Morse et al. (1995) interpreted their observations in terms of an expanding (1650 km s^{-1}) 10 pc ellipsoidal ejecta shell. Assuming undecelerated expansion, they estimated the remnant's age at 3150 yr, 10 times older than Cas A. Spectroscopy with *ASCA* (Hughes et al. 1998) and *XMM-Newton* (Behar et al. 2001) showed that the X-ray emission is dominated by the shocked ambient medium. X-ray emission from ejecta has not yet been convincingly demonstrated, although it might be expected based on the high (30–35 M_{\odot}) mass of the SN progenitor inferred from optical and UV spectroscopy (Blair et al. 2000). We report here the discovery of clumpy X-ray-emitting O ejecta in N132D with new *Chandra* X-ray observations, matching (on large scales) the optical ejecta morphology as seen by *Hubble*.

2. IMAGING

N132D was observed by the *Chandra X-Ray Observatory* on 2006 January 9, 10, and 16 with the Advanced CCD Imaging Spectrometer (ACIS) S3 CCD chip, at the same telescope roll angle and target location for each observation, for a total effective exposure of 89.3 ks. Data were processed with CIAO version 3.4 and CALDB 3.3.0 with default processing options. While the data were acquired in the very faint telemetry mode, we chose the default faint format in data analysis because of a significant loss of source photons in high surface brightness sections of the remnant with the very faint format. A large background region covering most of the S3 chip was used for all spectra. Spectral analysis was performed with XSPEC version 12 (Arnaud 1996). We used the nonequilibrium ionization (NEI) version 2.0 thermal models, based on the APEC/APED spectral codes (Smith et al. 2001) and augmented by addition of inner-shell processes (Badenes et al. 2006).

We obtained 2.8×10^6 source photons, with about 0.5% background. Images were smoothed using platelets with a default smoothing parameter $\gamma = 1/2$ (Willett 2007); Figure 1 (*top*) shows the remnant's X-ray morphology. We measured the position of a bright star visible in X-rays on the S3 chip to be within $0''.1$ of its USNO UCAC2 position.

High spatial resolution imaging of O-rich ejecta was done by the *Hubble Space Telescope* Wide Field Planetary Camera 2 (WFPC2; Morse et al. 1996) and the Advanced Camera for Surveys (ACS; Beasley et al. 2004). *Hubble* ACS images obtained on 2004 January 22 are most useful, because they provide a complete spatial coverage of the remnant, and the broad bandpass of the ACS Wide Field Channel (WFC) F475W filter includes [O III] $\lambda 5007$ emission from O ejecta even with most extreme radial velocities. In addition to the ACS F475W data, we also use ACS images taken with the F658N and F775W filters, to highlight the shocked ambient medium emitting strongly in H α and to distinguish diffuse SNR emission from numerous LMC stars. Individual ACS exposures (four per filter) were aligned and combined, and cosmic rays were removed with the on-the-fly reprocessing sys-

¹ Department of Physics, North Carolina State University, Raleigh, NC; kborkow@ncsu.edu.

² Department of Physics, Millersville University, Millersville, PA.

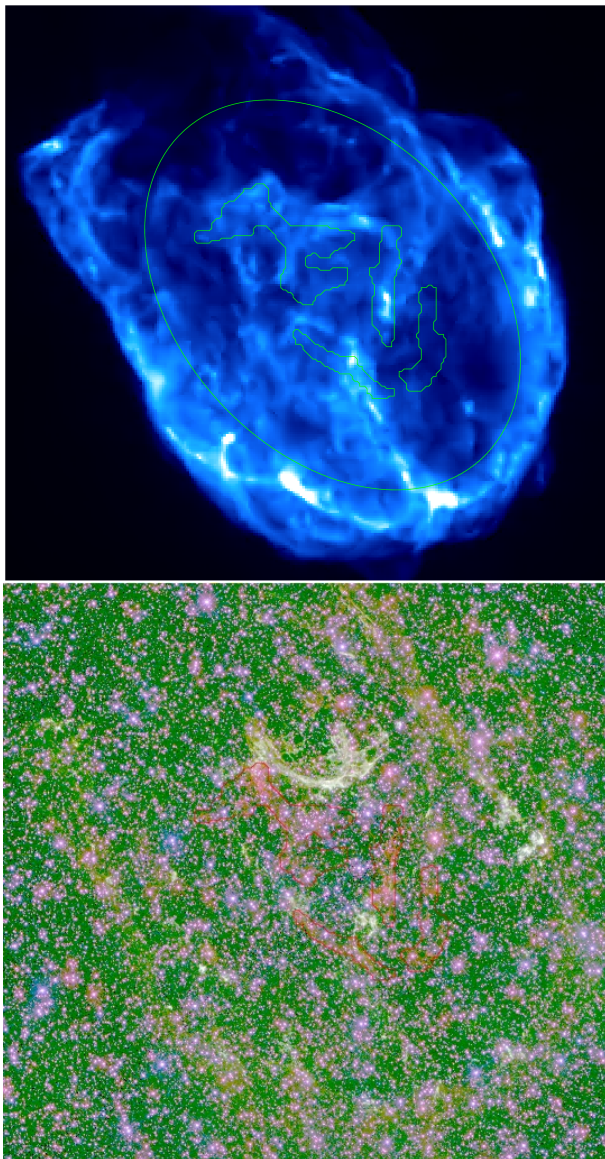


FIG. 1.— Top: *Chandra* ACIS image of N132D in the 0.3–7.0 keV energy range, smoothed with platelets (Willett 2007). The image is $120'' \times 115''$ in size. North is up and east is to the left. Note the complex filamentary structure within the remnant’s interior (enclosed by an ellipse) and the bright outer blast wave. Bottom: A three-color *Hubble* ACS image in F475W, F658N, and F775W filters (in red, green, and blue, respectively). O-rich ejecta are prominent in the F475W filter, while the shocked ISM radiates predominantly in the F658N filter (Beasley et al. 2004; see also a high quality image in Brown 2007, p. 26). The location of optically emitting O-rich ejecta is marked in both images.

tem at STScI. We refined the astrometric accuracy of the final combined images by identifying and measuring positions for a number of Guide Star Catalog II (GSC2) stars and shifting images from the GSC1 reference frame to the more accurate ($0''.3$) GSC2 frame. We present these images as a three-color image in Figure 1 (bottom); red diffuse emission marks the location of O-rich ejecta. We outline optically emitting O-rich ejecta, detected both in *Hubble* and in ground-based data of Morse et al. (1995), with solid lines in the bottom and top panels of Figure 1.

A similar approach allows us to locate O-rich ejecta in X-rays. We constructed a composite three-color image from soft (0.3–0.5 keV), medium (0.5–0.75 keV), and

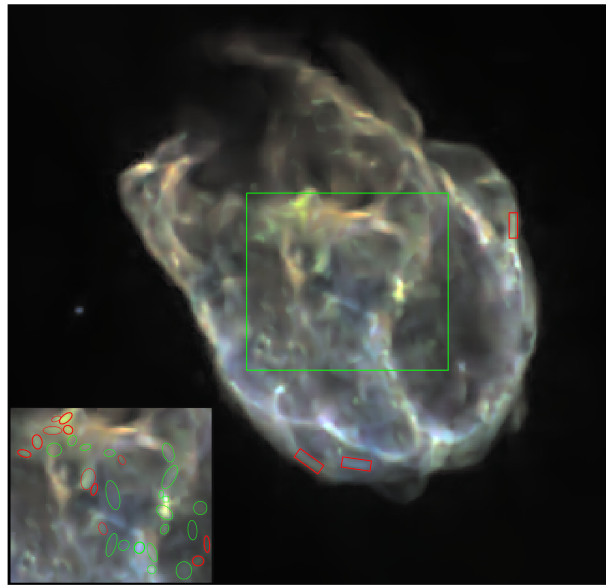


FIG. 2.— Merged image between 0.3 and 7 keV. Red: 0.3–0.5 keV; green: 0.5–0.75 keV; blue: 0.75–7 keV. All three images were smoothed using platelets (Willett 2007). X-ray knots and filaments near optical O-rich ejecta are shown in the inset. Red ellipses show ejecta knots and filaments with particularly strong emission in the O band (0.5–0.75 keV). Regions in green contain a mixture of ejecta and the shocked ambient medium. Three selected blast wave regions are enclosed by red rectangles.

hard (0.75–7 keV) energy bands (Fig. 2). Emission in the soft band is particularly sensitive to variations in the interstellar medium (ISM) absorption toward N132D. The medium band contains strong O He α 0.57 keV and O Ly α 0.65 keV lines; O-rich gas will produce an excess of emission in this band when compared with the ambient LMC gas. The broad hard band measures the strength of the overall X-ray emission. Figure 2 reveals widespread variations in X-ray colors in the central region. Enhancements in the medium band (*greenish knots and filaments*) correlate spatially with optical O-rich ejecta, implying O-rich X-ray-emitting ejecta with a similar large-scale distribution as the optical ejecta.

We attempted to quantify this spectral distinction between knots near optical O-rich ejecta and emission elsewhere in the interior. We selected a large number of X-ray emission enhancements in the N132D interior (within the ellipse shown in the top panel of Fig. 1, chosen to exclude the bright outer blastwave). This was done by repeated thresholding of the image shown in Figure 1 (top), filtered first by the unsharp masking procedure, and further processed with the morphology-based operation “opening” (a basic image-processing algorithm) to spatially separate partly overlapping emission enhancements. This procedure provided us with many spatial regions, preferentially sampling X-ray knots and filaments, as opposed to more spatially uniform inter-knot emission. Our final sample includes 145 regions.

We then counted photons within each region in unsmoothed *Chandra* images in each of the three energy bands, arriving at soft (*S*), medium (*M*), and hard (*H*) counts. We first examined regions not near O-rich ejecta, by excluding the regions shown in Figure 1. In Figure 3, we plot their colors $C_S = \log(S/H)$ and $C_M = \log(M/H)$. We also excluded regions with less than 16 counts (corresponding to a signal-to-noise ratio

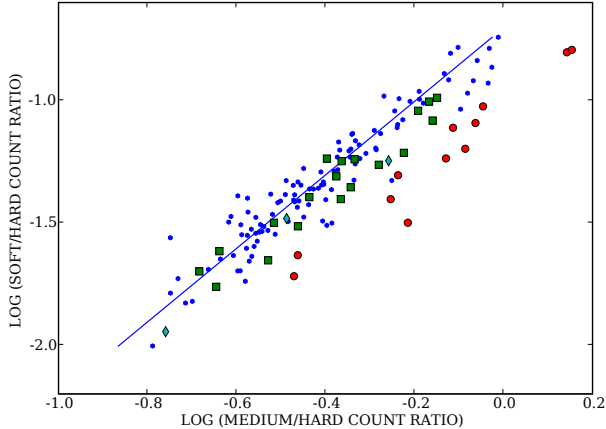


FIG. 3.— Color-color scatter plot, 0.3–0.5/0.75–7 vs. 0.5–0.75/0.75–7 keV count ratios (on log-log scale), for central regions of N132D (within the ellipse of Fig. 1, *top*). Colors of X-ray-emitting gas not overlapping spatially with O-rich optical ejecta cluster along a linear regression line with slope 3/2, while red and green regions associated with optical ejecta (Fig. 2) exhibit emission excess in the 0.5–0.75 keV band. Red circles denote regions with the most extreme colors, more than 3σ away from the regression line. Three outer blast wave regions are marked by diamonds.

$S/N < 4$) in the soft band, in order to reduce effects of counting (Poisson) noise. There is a large spread in X-ray colors in the center of N132D (Fig. 3), but they are strongly correlated. A linear regression describes this correlation well, and scatter about the regression line is dominated by the counting statistics in the soft band.

We next selected 31 X-ray emission enhancements located in close proximity to O-rich ejecta; they are shown in Figure 2. Their location in the color-color plot differs from the other central regions. While their colors are also strongly correlated, they show excess emission in the medium band (Fig. 3). Regions with the most extreme colors appear green in Figure 2; we marked them by large circles in Figure 3. The remaining regions appear blue; Figure 3 reveals that they still show an excess emission in the medium band. This excess emission indicates X-ray-emitting O-rich ejecta. The spatial distributions of optical and X-ray-emitting ejecta are strongly correlated, although a detailed comparison of Figures 1 (*bottom*) and 2 reveals that there is no exact correspondence between optical and X-ray emission on the smallest spatial scales. Clumpy X-ray-emitting ejecta have the same large-scale distribution as optically emitting ejecta, forming an expanding elliptical shell (Morse et al. 1995).

3. SPECTROSCOPY

In order to investigate the large spread in X-ray colors in N132D, we examined spectra of the blast wave at a number of locations along its periphery. We found substantial spatial variations in the ISM absorption, which greatly affect spectra at low photon energies. Three blast wave spectra in Figure 4 demonstrate this effect. We modeled them with a plane shock model (Borkowski et al. 2001), using a two-component (Galactic plus LMC) absorption. The Galactic absorption is $5.5 \times 10^{20} \text{ cm}^{-2}$ at the N132D location (based on H I radio observations of Staveley-Smith et al. 2003), while the intrinsic absorption N_H within the LMC was allowed to vary. We as-

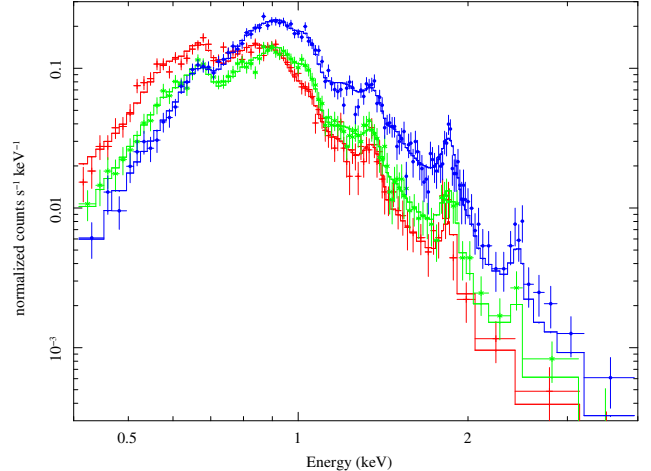


FIG. 4.— Spectra of the blastwave in three locations shown in Fig. 2, one in the west (*crosses*, red) and two in the south (*stars*, green; and *filled circles*, blue). Plane-shock model fits are shown by solid lines. Large spectral variations at low energies are caused by spatially varying absorption within the LMC.

sumed 0.4 solar abundances within absorbing LMC material, except for nitrogen, whose abundance is low (0.1 solar) in the LMC. The same abundances have been assumed for the emitting gas, except for Ne, Mg, and Fe (with Ni tied to Fe), whose abundances were allowed to vary. The best-fit value for N_H (LMC) of $1.4 \times 10^{20} \text{ cm}^{-2}$ ([0, 4] 90% confidence interval) in the western blast wave region is consistent with no absorption within the LMC, while significant absorption, $1.6(1.2, 2.1) \times 10^{21} \text{ cm}^{-2}$ and $4.1(3.6, 4.7) \times 10^{21} \text{ cm}^{-2}$ is required in the two southern regions. Plasma temperatures are nearly equal, 0.66, 0.71, and 0.67 keV, respectively—while ionization ages are longer in the south [$6.1(3.8, 8.4) \times 10^{11} \text{ cm}^{-3} \text{ s}$ and $15(8.7, 23) \times 10^{11} \text{ cm}^{-3} \text{ s}$] than in the west [$4.0(2.9, 5.3) \times 10^{11} \text{ cm}^{-3} \text{ s}$].

The X-ray colors of the blastwave depend strongly on N_H ; colors corresponding to spectra of Figure 4, and plotted in Figure 3, spread along the regression line. Colors become bluer down the line as absorption increases. We conclude that spatial variations in interstellar absorption are mostly responsible for the large range in X-ray colors seen in Figure 2. The significant difference in N_H between the two adjacent regions in the south demonstrates that absorption is clumpy on small spatial scales, although a large-scale north-south absorption gradient is also present. Banas et al. (1997) argued that N132D is physically associated with a molecular cloud located ~ 1.5 south of the remnant. While there is little spatial overlap between X-ray, CO, and H₂ emission (Banas et al. 1997; Tappe et al. 2006), Australia Telescope Compact Array H I 21 cm survey images (Kim et al. 2003) reveal the presence of substantial amounts of H I emission around this molecular cloud, extending to the northern tip of N132D. It is likely that this gas just outside the molecular cloud is responsible for the patchy X-ray absorption.

Spectra of several regions associated with optically emitting O-rich ejecta and with excess emission in the medium band are shown in Figure 5. These regions are marked by thick red ellipses in Figure 2; we added spectra for adjacent regions if their colors were similar. The

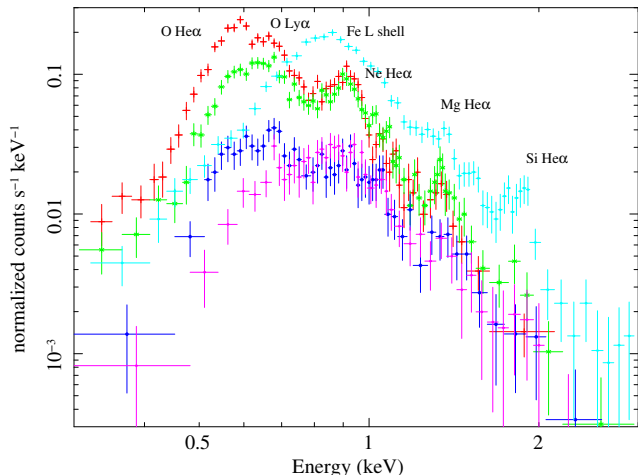


FIG. 5.— X-ray spectra of ejecta in four locations shown in Fig. 2 by thick red ellipses (we added spectra from adjacent ellipses in order to improve S/N ratio). For comparison, an X-ray spectrum of the shocked ambient gas is also shown (Fig. 2, *thick green ellipse*). From top to bottom (at 0.6 keV): North, east, ambient, west, and central spectra, with colors (C_M , C_S) equal to (0.15, -0.80), (-0.10, -1.14), (-0.64, -1.62), (-0.17, -1.34), and (-0.47, -1.72), respectively. Prominent X-ray lines are labeled. Oxygen lines in ejecta spectra are stronger than in the blast wave spectrum.

top spectrum corresponds to two northern knots with extremely soft hardness ratios (these knots are located in the top right corner of Figure 3). Bright optically emitting O-rich ejecta filaments overlap spatially (Morse et al. 1995) at the location of the northern knots. Strong O lines dominate the X-ray spectrum; they are much stronger than O lines in the blast wave spectra of Figure 4. The O He α line of the He-like O $^{+6}$ ion is stronger than the O Ly α line of the hydrogenic O $^{+7}$ ion. It is likely that a lower than average ionization state of O accounts for the softness of the X-ray spectrum. Spectra of ejecta in the east and west, corresponding to the blueshifted filaments B4 and B1 of Morse et al. (1995), also show strong O lines. These are most typical of ejecta spectra in N132D. The O Ly α line is now stronger than the O He α line, resulting in harder spectra and bluer X-ray colors. The X-ray colors of the eastern knots place them in the main “clump” of ejecta knots in the X-ray color-color plot (Fig. 3), significantly below the color-color relationship for the shocked ambient gas. The X-ray spectrum of a small central ejecta knot (the bottom spectrum in Fig. 5) corresponds to even bluer X-ray colors ($C_M = -0.47$, $C_S = -1.72$). A comparison with the hard ($C_M = -0.64$, $C_S = -1.61$) spectrum of a bright interior knot with the normal (LMC) abundance (Fig. 5) reveals the presence of stronger than average O lines, but they are weaker than in other ejecta spectra, likely because of the increased absorption. A substantial amount of absorbing LMC gas appears to be present toward the very center of N132D; a central “blue hole” seen in Figure 2 corresponds to an absorbing ISM cloud with $N_H(\text{LMC}) = 3 \times 10^{21} \text{ cm}^{-2}$.

Strong O lines in ejecta spectra may be due either to enhanced O abundances or to short ionization ages. We fit the top spectrum of Figure 5 with a plane shock model with temperature of 0.59 keV and ionization age of $4 \times 10^{10} \text{ cm}^{-3} \text{ s}$ and with nearly the same abundances as in the blast wave. For electron densities of $> 15 \text{ cm}^{-3}$

(typical of the N132D blast wave; Williams et al. 2006), the very short ionization age implies a shock age of less than 100 yr. This is clearly an unreasonably short shock age for a 3000 yr old SNR. Problems arise also if low ($\sim 1 \text{ cm}^{-3}$) electron densities are assumed, as such low-density gas with LMC abundances is too faint in X-rays. This would also require a substantial (an order of magnitude or more) pressure imbalance between the ejecta and the blast wave, rather difficult to sustain for a prolonged period of time. These severe difficulties suggest that the alternative explanation of strong O lines in terms of O-rich ejecta is the correct one. The determination of plasma conditions and abundances within the ejecta would require a separate, detailed spectroscopic analysis involving a superposition of heavy-element ejecta and blast wave emission. We just note here that the low O Ly α /O He α line ratio of 0.41 (0.36 after correction for absorption) in the plane shock fit just mentioned implies a low (0.2 keV) plasma temperature under conditions of collisional ionization equilibrium expected in dense shocked O-rich ejecta clumps. It is likely the observed clumpy ejecta emission arises in relatively dense O-rich ejecta, which have been shocked by low-velocity shocks propagating into O-rich clumps. We estimate that a few tenths of M_\odot of O is present in these clumps.

4. DISCUSSION

High spatial resolution imaging and spectroscopy of N132D with *Chandra* reveal the presence of clumpy O-rich ejecta in its center. The spatial distribution of X-ray-emitting ejecta correlates well with optically emitting ejecta on large (but not small) scales. This shows that optical and X-ray emission can be closely linked in dynamically advanced remnants such as N132D, where most of the O might have already been shocked. In N132D, ejecta are located in an expanding ellipsoidal shell. No such shell is present in either G292.0+1.8 or Pup A, two O-rich Galactic SNRs with ages similar to N132D. Optically emitting ejecta in G292.0+1.8 are distributed throughout much of the remnant, with little detailed correlation with X-rays (Winkler & Long 2006). Asymmetrically distributed optical ejecta filaments in Pup A are moving in the opposite direction to its neutron star (Winkler & Petre 2007). This demonstrates that the innermost metal-rich ejecta are strongly affected by poorly understood processes leading to CC explosions. No correlation of optical emission with more evenly distributed X-ray-emitting ejecta has been reported. X-ray expansion velocities in N132D are poorly known; Hwang et al. (1993) found (marginal) evidence for an X-ray expansion consistent with the optical expansion in spatially integrated spectra obtained by *Einstein*, but archival *Chandra* and *XMM-Newton* grating spectra are more suitable for studying the ejecta kinematics. The origin of the X-ray and optically emitting ejecta shell is unknown at this time. It may be the location of a reverse shock propagating into ejecta; more likely, it may be an ejecta shell created by a Ni bubble effect shortly after the SN explosion, similar to what is seen in the O-rich SNR B0049-73.6 (Hendrick et al. 2005). More detailed analysis of existing *Chandra* and *XMM-Newton* observations is warranted.

We thank Paul Plucinsky for help planning the *Chan-*

dra observations. This work was supported by NASA through grants SAO G05-6053A and SAO G05-6053B.

REFERENCES

- Arnaud, K. A. 1996, in *Astronomical Data Analysis and Systems V*, eds. G. Jacoby & J. Barnes, ASP Conf. Series, v.101, 17
- Badenes, C., et al. 2006, *ApJ*, 645, 1373
- Banas, K. R., et al. 1997, *ApJ*, 480, 607
- Beasley, M., et al. 2004, *BAAS*, 36, 1510
- Behar, E. et al. 2001, *A&A*, 365, L242
- Blair, W. P., et al. 2000, *ApJ*, 537, 667
- Borkowski, K.J., Lyerly, W.J., & Reynolds, S.P. 2001, *ApJ*, 548, 820
- Brown, R., ed. 2007, *Hubble 2006: Science Year in Review* (Baltimore: STScI)
- Hendrick, S. P., Reynolds, S. P., & Borkowski, K. J. 2005, *ApJ*, 622, L117
- Hughes, J. P., Hayashi, I., & Koyama, K. 1998, *ApJ*, 505, 732
- Hwang, U., et al. 1993, *ApJ*, 414, 219
- Kim, S., et al., 2003, *ApJS*, 148, 473
- Morse, J. A., et al., 1996, *AJ*, 112, 509
- Morse, J. A., et al., 1995, *AJ*, 109, 2104
- Smith, R. K., et al. 2001, *ApJ*, 556, L91
- Staveley-Smith, L., et al. 2003, *MNRAS*, 339, 87
- Sutherland, R. S., & Dopita, M. A. 1995, *ApJ*, 439, 365
- Tappe, A., Rho, J., & Reach, W. T. 2006, *ApJ*, 653, 267
- Willett, R. 2007, in *Statistical Challenges in Modern Astronomy IV*, ed. Feigelson & Babu (APS Conf. Ser., in press)
- Williams, B. J., et al. 2006, *ApJ*, 652, L33
- Winkler, P. F., & Long, K. S. 2006, *AJ*, 132, 360
- Winkler, P. F., & Petre, R. 2007, *ApJ*, 670, 635